Volume 12
Number 47
21 December 2021
Pages 6783-6954

Polymer Chemistry

rsc.li/polymers

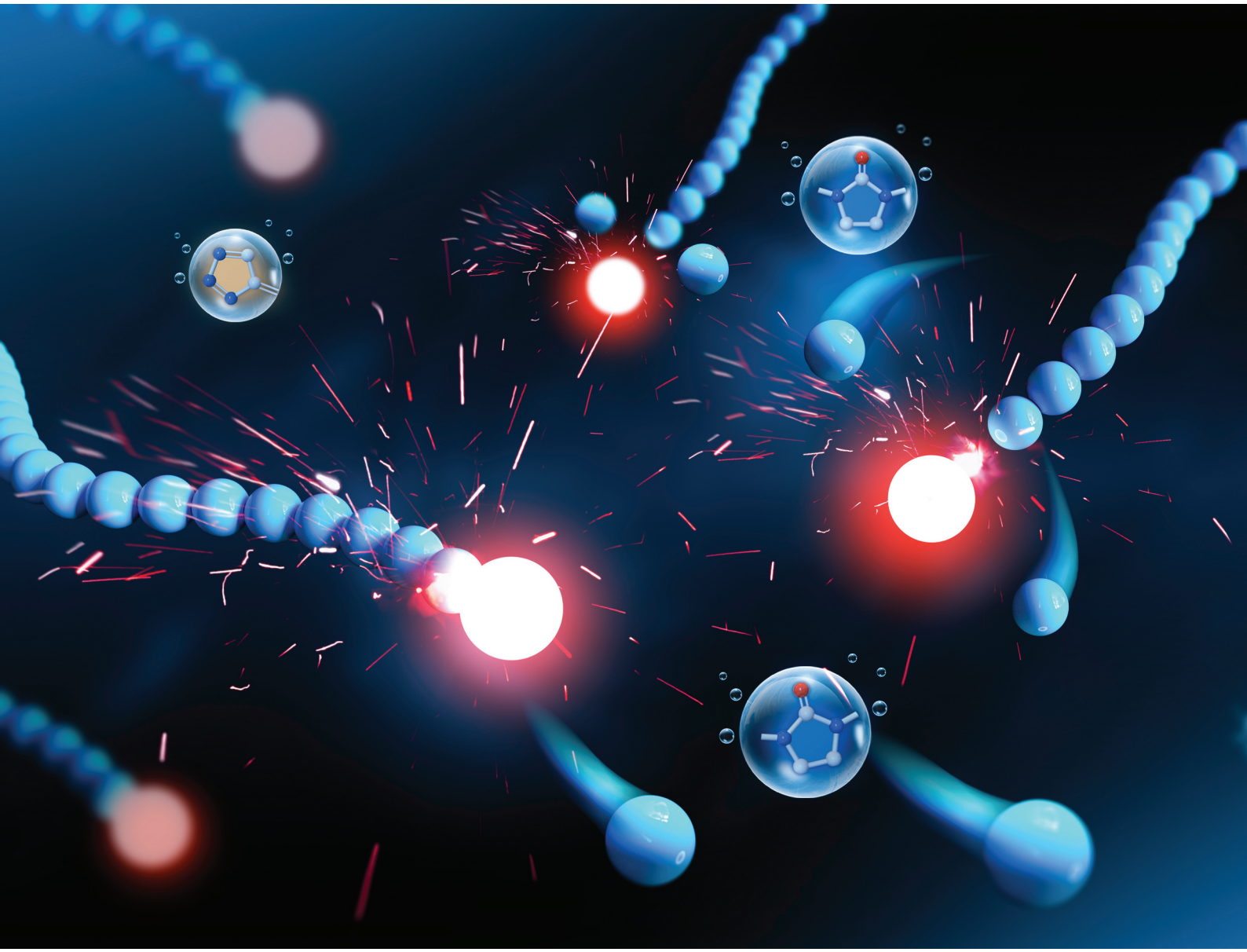

ISSN 1759-9962

ROYAL SOCIETY OF CHEMISTRY

PAPER
Elizabeth R. Gillies, Derrick A. Roberts *et al.*
Post-polymerization 'click' end-capping of polyglyoxylate self-immolative polymers

Polymer Chemistry

ROYAL SOCIETY OF CHEMISTRY

PAPER

View Article Online
View Journal | View Issue

Cite this: *Polym. Chem.*, 2021, **12**, 6824

Post-polymerization 'click' end-capping of polyglyoxylate self-immolative polymers†

Peter G. Maschmeyer, [a] Xiaoli Liang, [b] Allison Hung, [b] Oksana Ahmadzai, [a] Annmaree L. Kenny, [a] Yuan C. Luong, [a] Timothy N. Forder, [a] Haoxiang Zeng, [a] Elizabeth R. Gillies *[b,c] and Derrick A. Roberts *[a,d]

Received 29th August 2021,
Accepted 24th September 2021

DOI: 10.1039/d1py01169c

rsc.li/polymers

Post-polymerization modification is a powerful tool for expanding the functionality and tuning the properties of self-immolative polymers (SIPs), typically through reactions of the polymer repeat units. Herein, we investigate the use of post-polymerization 'click' reactions to attach stimuli-responsive end-caps to poly(ethyl glyoxylate) (PEtG) SIPs. Two classes of alkyne-terminated polymers were synthesized, with the alkyne attached to the PEtG either by an acetal or carbonate bridge. These PEtGs were treated with azide-functionalized self-immolative linker precursors *via* the copper(I) catalyzed azide–alkyne cycloaddition reaction to afford PEtGs end-capped with cleavable self-immolative triazole (SIT) linkers. Our results demonstrate that degradation of the PEtGs can be initiated by cleavage of the SIT end-caps, and that successful cleavage depends strongly on the moiety that connects the SIT linker to the PEtG backbone. Through depolymerization studies on the polymers and a series of small molecule model compounds, we examined in detail the mechanistic features of this system. Additionally, we demonstrate that this modular chemistry is versatile for introducing different stimuli-responsive end-caps to a single pre-synthesized PEtG.

Introduction

Linear self-immolative polymers (SIPs) are degradable macromolecules that undergo complete head-to-tail depolymerization following the cleavage of the backbone or a single stimuli-responsive end-cap (designated as the 'trigger' group).[1] This contrasts with the behavior of most conventional degradable polymers, whereby the cleavage of one bond does not typically drive the cleavage of adjacent bonds (Scheme 1). SIPs naturally function as chemical amplifiers of weak triggering signals, with a single bond cleavage event releasing multiple degradation products.[2] Additionally, a wide range of trigger end-caps have been reported to date, allowing SIPs to degrade in response to various environmental, chemical, and biological stimuli.[3] These unique properties of SIPs have fueled interest for their use in controlled release systems,[4–10] stimuli-responsive coatings,[11,12] chemical sensors,[13–15] and degradable bulk materials.[16–18]

Since their debut in 2008,[19] a handful of SIP designs have been reported with degradation mechanisms based on 1,4- and 1,6-elimination reactions of aromatic compounds,[20–22] heterocyclization reactions,[23,24] olefin sulfone elimination reactions,[25–27] and the depolymerization of polyacetals.[28,29] While each of these designs have reliable polymerization methods, functional group intolerances preclude the direct polymerization of certain monomers. To circumvent this issue, post-polymerization modification (PPM) has become an impor-

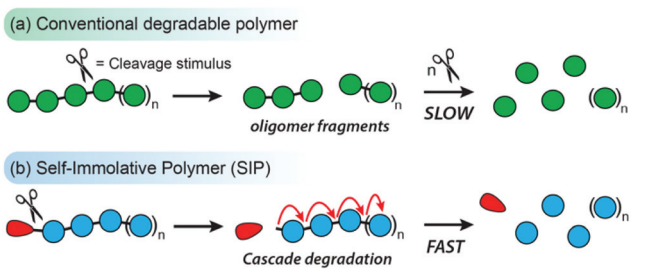

Scheme 1 Comparison of (a) conventional degradable polymers, which tend to undergo stepwise fragmentation through random bond scission events; and (b) a linear end-capped SIP, which undergoes a head-to-tail depolymerization cascade upon removal of a single 'trigger' end-cap (red circle).

[a]*Key Centre for Polymers and Colloids, School of Chemistry, The University of Sydney, Sydney, NSW 2006, Australia. E-mail: derrick.roberts@sydney.edu.au*
[b]*Department of Chemistry and the Centre for Advanced Materials and Biomaterials Research. The University of Western Ontario, 1151 Richmond St., London, Canada N6A 5B7. E-mail: egillie@uwo.ca*
[c]*Department of Chemical and Biochemical Engineering, The University of Western Ontario, 1151 Richmond St., London, Ontario, Canada N6A 5B9*
[d]*Sydney Nano Institute, The University of Sydney, Sydney, NSW 2006, Australia*
†Electronic supplementary information (ESI) available. See DOI: 10.1039/d1py01169c

tant tool for introducing functional groups to SIPs that would otherwise interfere with their polymerization reactions. For example, Shabat and co-workers have shown that protecting groups can mask nucleophilic functionalities *en route* to water soluble poly(benzyl urethanes).[30] Zhang and co-workers have used post-synthetic disulfide metathesis[31] and 'click'-type reactions[32] to prepare SIP bottlebrushes and organogels. Gillies and co-workers have developed PPM strategies for preparing a range of functionalized polyglyoxylate and polyglyoxylamide SIPs *via* transesterification[33] and amidation reactions,[34] which significantly expand the functional scope of these polymers. Furthermore, PPM has been used to prepare block copolymers from both linear and branched SIPs.[28,35–37]

In addition to avoiding functional group incompatibilities, PPM also enables rapid derivatization of a single parent macromolecule, which can be useful for tuning chemical functionality and physical properties.[38–43] While strategies for modifying the repeat units of SIPs have been explored previously, there are no reported approaches for introducing triggerable end-caps to an existing SIP backbone *via* PPM. In addition to being a fundamentally interesting pursuit, such a capability could also provide a modular route for varying the stimuli-responsivity of a pre-formed SIP through late-stage introduction of different trigger end-caps.

Recently, Roberts and co-workers developed a method for preparing self-immolative triazole (SIT) linkers using the copper(I) catalyzed azide–alkyne cycloaddition (CuAAC) 'click' reaction,[44] and have demonstrated its suitability for the post-synthetic modification of RAFT polymers.[45] A key feature of this linker design is that the triazole group plays an active role in the self-immolation cascade and allows rate-tuning of the degradation kinetics through substituent effects. These features led us to hypothesize that a SIT linker, if attached to the end of a SIP, could offer a convenient way to introduce different trigger end-caps through PPM. To test this hypothesis, we investigated the post-synthetic 'click' activation of alkyne-terminated poly(ethyl glyoxylate)s (PEtGs) using two exemplar azide capping groups, and studied their degradation behavior by *in situ* ^{1}H NMR spectroscopy (Scheme 2). Through this investigation, we show that a SIT cap can be successfully 'clicked' onto the terminus of a PEtG without causing incipient depolymerization. Additionally, self-immolation can successfully proceed *via* the degradation of the SIT linker for certain end-cap structures. Furthermore, we explore the interesting finding that the rate of SIT end-cap self-immolation is not sensitive to substituent effects when attached to the terminus of PEtG, contrary to the behavior of previously reported SIT linker systems.

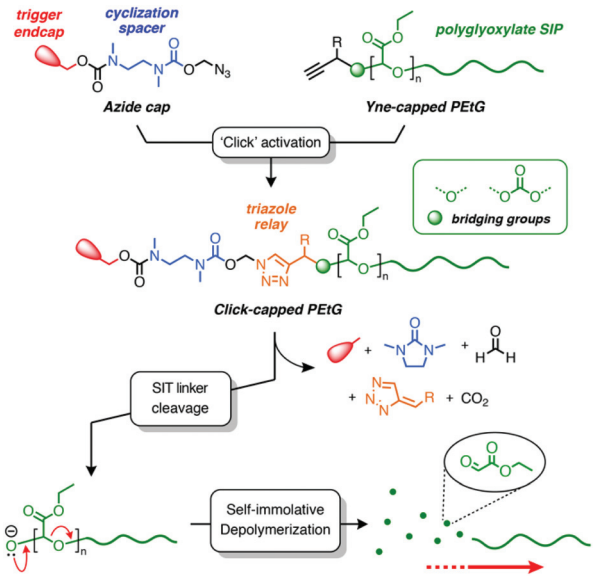

Scheme 2 Overview scheme summarizing our approach for the post-synthetic 'click' activation of PEtG SIPs with self-immolative triazole (SIT) linkers. Structure–property relationships are explored by varying the bridging group (acetal or carbonate) and triazole Cα-substituent (R) then examining the effect these changes have on the kinetics of SIT linker degradation and overall depolymerization.

Results and discussion

Polymer synthesis and 'click' activation

Alkyne-terminated PEtGs **P1a–b** and **P2a–b** (Scheme 3a and Table 1) were prepared by the anionic polymerization of ethyl glyoxylate.[46] To prepare **P1a–b**, the polymerization reactions were initiated with the corresponding alkoxides of propargyl alcohol or but-3-yn-2-ol after their deprotonation by *n*-butyllithium (*n*-BuLi), and the resulting PEtGs were end-capped with benzyloxymethyl chloride (Scheme 3a). **P2a–b** were synthesized by direct initiation of the polymerization with *n*-BuLi and end-capping with either propargyl chloroformate or the chloroformate prepared from 3-butyn-2-ol (Scheme 3b). All PEtGs had peaks corresponding to their expected termini in their ^{1}H NMR spectra (ESI, section S3†). Their number average molar masses (M_n) ranged from 4–10 kg mol^{-1} based on size exclusion chromatography (SEC) and their dispersities ($Đ$) ranged from 1.2–1.3 (Table 1). As a result of their polymerization mechanisms, each set of polymers has a different bridging moiety linking the propargyl end-group to the polymer backbone; **P1a–b** are acetal-bridged, while **P2a–b** are carbonate-bridged. Additionally, the use of propargyl *versus* but-3-yn-2-ol allows us to investigate how substitution at the carbon atom adjacent to the triazole 4-position (henceforth referred to as the Cα-position) influences the rate of depolymerization, since this has been shown to influence 1,4-elimination rates in related SIT linkers.[44,47] Syntheses of alkyne-capped PEtGs with geminal methyl groups at the propargylic position were attempted, but failed to give the desired polymers, most likely due to a combination of steric factors and possibly decomposition of 2-methylbut-3-yn-2-ol under basic conditions.[48]

Post-synthetic 'click' activation of PEtGs **P1a–b** and **P2a–b** was initially investigated using allyl-protected cap **A1**, which has served as a reliable and conveniently studied model cap in previous work.[44,45] Alkyne-terminated PEtGs were treated with azide **A1** (1.5–2.0 equiv.) in DMF at 50 °C under CuAAC con-

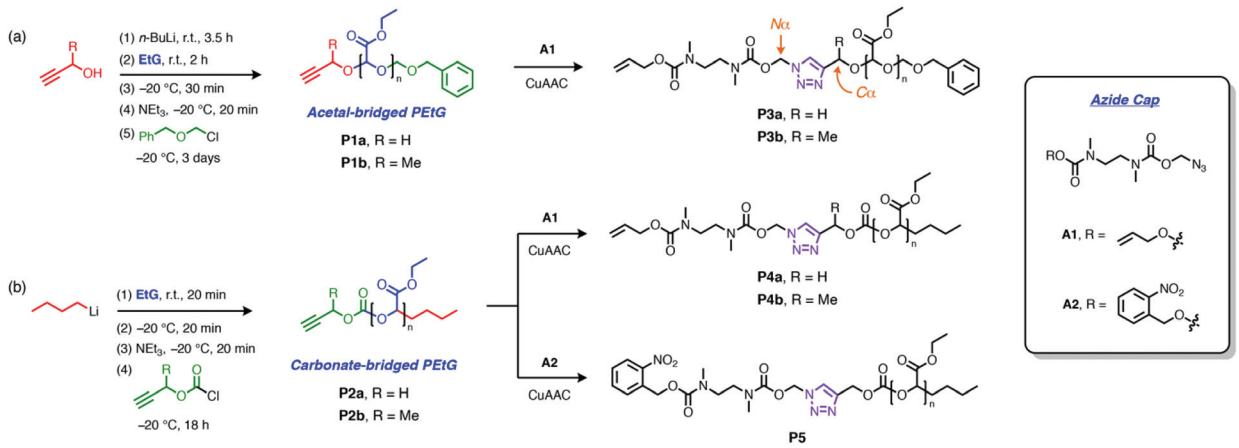

Scheme 3 Synthesis and post-synthetic capping of alkyne-terminated PEtGs. (a) Synthesis of acetal-bridged PEtG derivatives. The Nα and Cα positions adjacent to the triazole ring are annotated on **P3a–b**. (b) Synthesis of carbonate-bridged PEtG derivatives. CuAAC Conditions: $CuSO_4{\cdot}5H_2O$ (0.3 equiv.), sodium ascorbate (0.9 equiv.), DMF, 50 °C, 16–24 h.

Table 1 Characterization data for alkyne-capped precursor and 'click'-capped product PEtGs. M_n values are given in kg mol^{-1}. $M_{n,NMR}$ values are estimated by end-group integration analysis. See ESI† for full characterization data

Entry	$M_{n,NMR}$	DP_{NMR}	$M_{n,SEC}$	$Đ$
P1a	5.4	51	4.0	1.32
P1b	11.1	107	10.3	1.17
P2a	4.3	41	5.3	1.31
P2b	3.8	36	4.7	1.27
P3a	5.1	46	3.9	1.37
P3b	12.3	116	10.4	1.12
P4a	4.2	37	5.7	1.27
P4b	3.0	25	4.0	1.36
P5	5.9	53	6.9	1.21

ditions using a copper(II) sulfate and sodium ascorbate catalyst system. Reaction mixtures were heated for 16–24 h, then dissolved in EtOAc and washed with aqueous Na_2EDTA to remove copper salts. Excess **A1** was removed by dissolving the polymers in CH_2Cl_2 followed by dropwise addition of Et_2O, resulting in precipitation of the polymers. Upon vacuum drying, alloc-capped PEtGs **P3a–b** and **P4a–b** were obtained as tacky solids. Successful introduction of the SIT caps was confirmed by ^{1}H NMR spectroscopic analyses, which showed peaks characteristic of the attached SIT linker in all cases (ESI, section S4†). DOSY NMR spectroscopy also showed that the end-group and polymer backbone resonances shared similar diffusion coefficients, further supporting successful post-synthetic capping of the PEtGs. SEC traces of polymers **P3a–b** and **P4a–b** did not change appreciably following CuAAC modification and purification (Table 1).

Kinetics I: acetal-bridged PEtGs

Palladium(0)-triggered degradation of **P3a–b** was studied by ^{1}H NMR spectroscopy in DMSO-d_6/D_2O (9 : 1) at 65 °C in the presence of morpholine (10 equiv.) to regenerate the catalyst and assist with base-mediated fragmentation of the SIT linker. This solvent mixture was chosen to demonstrate the compatibility of the linker with the presence of water; however, solubility limitations precluded higher aqueous fractions. A control experiment showed that the polymers were stable towards morpholine in the absence of catalyst (ESI, section S9.2†). Self-immolation was initiated by addition of $Pd(PPh_3)_4$ (0.2 equiv. per trigger) to an NMR tube containing the polymer solution. Broad ^{1}H resonances of the PEtG obscured peaks of the allyl end-cap and Cα-environment, preventing direct observation of trigger cleavage and 1,4-elimination for both polymers. However, the progress of subsequent diamine cyclization could be tracked by monitoring loss of the *N*α-methylene group adjacent to the triazole ring and the concomitant appearance of the cyclization product 1,3-dimethyl-2-imidazolidinone (DMI) (Scheme 4b). For both **P3a** and **P3b**, complete cyclization of the spacer occurred within 25 min (Scheme 4b). However, in both cases the integral of the PEtG backbone did not decrease appreciably even after 3 h at 65 °C, and peaks corresponding to the hydrated PEtG degradation product, ethyl glyoxylate hydrate (EtGH), were not observed. These results suggest that degradation of the SIT linker was interrupted, presumably due to unsuccessful 1,4-elimination of the triazole moiety, thereby preventing degradation of the polymer backbone.

We prepared acetal-bridged model compounds **1a–c** (Scheme 5a) to better understand why polymers **P3a–b** did not undergo complete self-immolation. These model compounds have much simpler NMR spectra than the corresponding polymers, which enabled more detailed analysis of their degradation profiles. Additionally, geminal dimethyl-substituted **1c** was successfully synthesized, providing an additional congener for studying the potential influence of *C*α-substitution on the self-immolation kinetics.

Self-immolation reactions of **1a–c** were performed under slightly more forcing conditions than **P3a–b** (50 equiv. morpholine in DMSO-d_6/D_2O 8 : 2, 65 °C) to ascertain if 1,4-elimin-

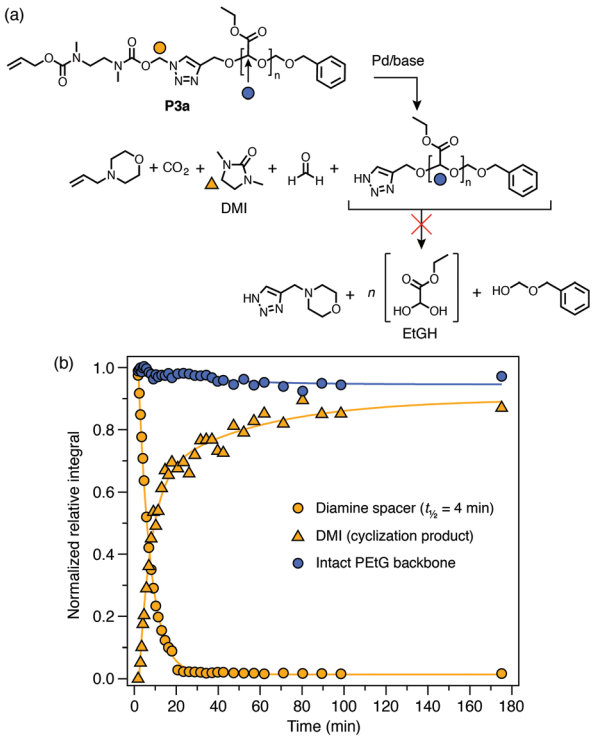

Scheme 4 Representative degradation profile of polymer **P3a**. Full data included in the ESI (section S9.2†). (a) Scheme depicting the proposed degradation pathway. Markers denote ^{1}H environments monitored for kinetics. (b) Degradation plot, measured by ^{1}H NMR (~10 mmol in DMSO-d_6/D_2O 9 : 1, 65 °C; 10 equiv. morpholine) showing complete cyclization of the diamine spacer, but no appreciable decrease in the integral of peaks representing the PEtG backbone. Diamine cyclization was modelled as a first-order process to estimate its half-life.

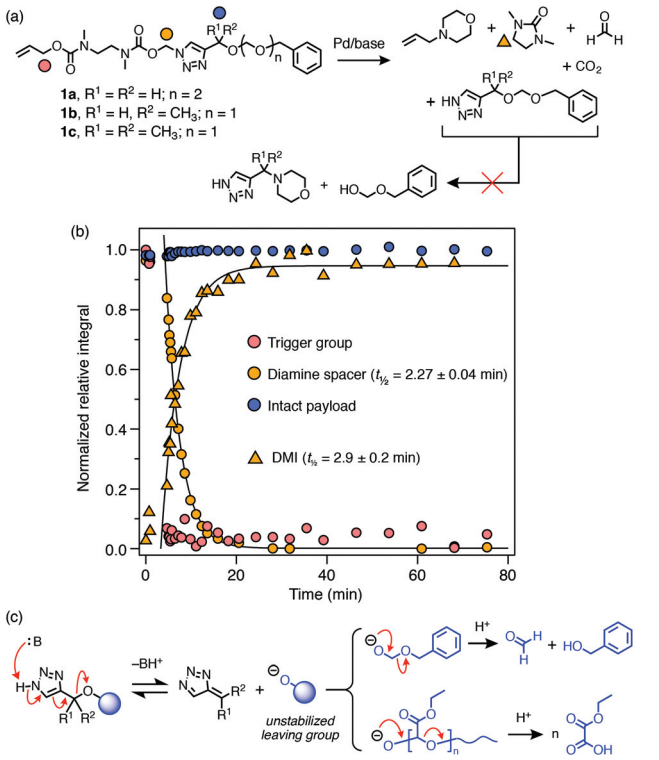

Scheme 5 Self-immolation of acetal-bridged model compounds. (a) Degradation reaction scheme for **1a–c**. Markers denote ^{1}H environments monitored for kinetics. (b) Representative degradation profile of **1c**, measured by ^{1}H NMR (25 mM in DMSO-d_6/D_2O 8 : 2, 65 °C; 50 equiv. morpholine). Half-lives were estimated by approximating the degradation profiles as first-order processes. (c) Scheme illustrating the putative 1,4-elimination products of acetal-bridged SIT derivatives, which would result in the formation of an unstable deprotonated hemiacetal anion before further stepwise fragmentation.

ation was possible with the acetal-bridged linker design. Following Pd(0) addition, trigger cleavage and diamine cyclization were complete within 25 min for all three compounds (Scheme 5b; ESI, section S9.2†). However, in all cases 1,4-elimination of the triazole moiety was not observed, which agrees with the behavior of **P3a–b**. Failure of the triazole groups to undergo 1,4-elimination, even under ostensibly more favorable conditions, suggests that the acetal bridge has a high barrier to elimination irrespective of the degree of substitution at the Cα-position. We attribute this barrier to poor leaving group ability of the deprotonated hemiacetal elimination product that would result from scission of the triazolylmethoxy C–O bond (Scheme 5c). For the PEtGs, the subsequent depolymerization cascade was expected to provide a thermodynamic driving force that would encourage 1,4-elimination across the triazole ring. However, this hypothesis was not supported by our observations.

Kinetics II: carbonate-bridged PEtGs

Next, carbonate-bridged polymers **P4a–b** were investigated. These polymers were expected to be more amenable to degradation due to the enhanced leaving group ability of the carbonate, as well as the irreversible expulsion of CO_2 upon 1,4-elimination. To test this hypothesis, **P4a–b** were subjected to the same degradation conditions as the previous polymers, undergoing rapid trigger cleavage upon addition of $Pd(PPh_3)_4$, followed by cyclization of the diamine spacer (Scheme 6b; ESI, section S9.3†). In both cases, signals of the PEtG backbone were also observed to decrease, indicating successful depolymerization that reached ~80% degradation after 2 h. Interestingly, cyclization of the diamine spacer in **P4a–b** was significantly slower than for the acetal-bridged polymers and model compounds, which we attribute to a reversible side-reaction between the deprotected diamine spacer and ethyl glyoxylate to form a transient hemiaminal species (see ESI, section S10,† for auxiliary discussion). A catalyst-free control experiment for **P4a** revealed that the PEtG backbone undergoes a small degree of background degradation (Scheme 6c) *via* base hydrolysis of the carbonate bridge. However, background degradation is considerably slower than triggered self-immolation, indicating that they are distinct processes. Thus, successful degradation of **P4a–b** demonstrates that the carbonate bridge functions as a better leaving group for triazole 1,4-elimination than the acetal analogue.

An interesting feature in the degradation profiles of **P4a–b** is the simultaneous rates of diamine cyclization and depoly-

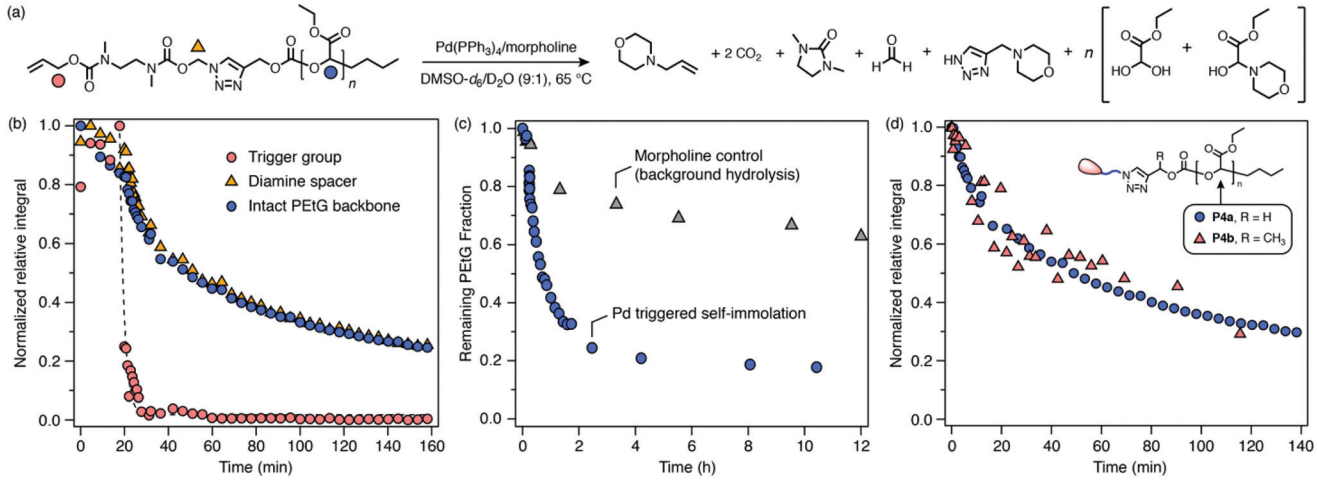

Scheme 6 Representative degradation kinetics of **P4a**. Degradation profiles were measured by ^{1}H NMR (~10 mmol in DMSO-d_6/D_2O 9 : 1, 65 °C; 10 equiv. morpholine) (full data included in ESI, section S9.3†). (a) Proposed degradation pathway. Markers denote the proton environments monitored in (b). (b) Degradation profile showing rapid trigger cleavage, then simultaneous cyclization and depolymerization steps. (c) Comparison of background hydrolysis and depolymerization profiles of **P4a** over 10 h. The integral of the PEtG acetal CH environment was monitored in both cases. (d) Comparison of depolymerization profiles of **P4a** and **P4b**, showing that the depolymerization is not sensitive to the *C*α-substituent.

merization (Scheme 6b; ESI Fig. S65†), which indicates that cyclization of the SIT linker is the rate-determining step of the overall cascade. Moreover, the normalized depolymerization profiles of **P4a** and **P4b** are nearly identical despite having different *C*α-substituents (Scheme 6d), which also suggests that triazole 1,4-elimination is not rate-determining. This contrasts with the behavior of previously reported carbamate-bridged SIT linkers,[44] for which 1,4-elimination is generally the slowest self-immolation step.

The high rate of 1,4-elimination relative to cyclization for **P4a–b** is consistent with carbonate being a better leaving group than a carbamate or a deprotonated hemiacetal. To verify this observation, we prepared model compounds **2a–b** and examined their degradation profiles under the same conditions as **P4a–b** (DMSO-d_6/D_2O 9 : 1, 65 °C, 10 equiv. morpholine). Both compounds exhibited identical cyclization rates (Scheme 7) that agreed closely with cyclization rates for the acetal-bridged compounds ($t_{\frac{1}{2}} \sim 3$ min). The rates of 1,4-elimination were either concomitant with (**2b**) or slightly slower (**2a**) than cyclization, demonstrating that the carbonate bridge is an excellent leaving group. Interestingly, the control experiment for **2a** also revealed that the carbonate bridge was completely stable for at least 1 h both in DMSO-d_6/D_2O (9 : 1) with 10 equiv. morpholine, and DMSO-d_6/D_2O (8 : 2) with 50 equiv. morpholine (ESI, section S9.3†). This result suggests that background hydrolysis observed for **P4a–b** may be partly driven by the large increase in entropy upon depolymerization.

Kinetics III: light-cleavable SIT-cap

Kinetics results for the carbonate-bridged compounds demonstrated that their degradation is largely insensitive to substitution at the Cα-position. A fortunate consequence of this insensitivity is that the least hindered alkyne-PEtG precursor (**P2a**) can be used as a parent compound for other post-syn-

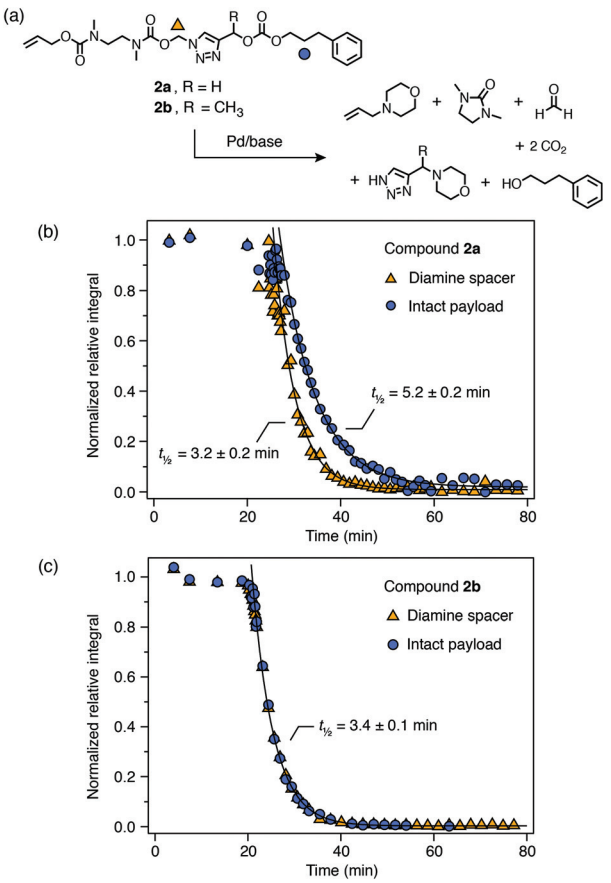

Scheme 7 Self-immolation of carbonate-bridged model compounds measured by ^{1}H NMR spectroscopy (25 mM in DMSO-d_6/D_2O 9 : 1, 65 °C; 10 equiv. morpholine). Half-lives were estimated by modelling the degradation profiles as first-order processes. (a) Proposed degradation reaction for **2a–b**. Markers denote ^{1}H environments monitored for kinetics (circles for **2a** and diamonds for **2b**). (b) Degradation profile of **2a**. (c) Degradation profile of **2b**.

thetic activation reactions. To demonstrate the versatility of this method, we synthesized novel azide linker **A2**, which carries an *o*-nitrobenzyl carbamate trigger group that can be cleaved by UV photoirradiation (Scheme 8). Treatment of **P2a** with **A2** under CuAAC conditions afforded 'click'-activated derivative **P5**. As for the other 'click'-activated polymers, ^{1}H NMR and DOSY spectroscopy confirmed successful attachment of the SIT linker and SEC analysis showed that there were no substantial changes in the molecular weight distribution of the polymer (ESI, section S8†).

Self-immolation of **P5** was initiated by irradiating a solution of the polymer in DMSO-d_6/D_2O (9 : 1) at 365 nm for 30 min, followed by incubation at 65 °C. The *o*-nitrobenzyl group was completely cleaved within this 30 min window as confirmed by ^{1}H NMR spectroscopy (ESI, Fig. S73†). Subsequent *in situ* ^{1}H NMR monitoring showed successful cyclization of the diamine linker and depolymerization of the PEtG backbone, with cyclization being the rate-determining step, as was observed for **P4a–b**. A negative control experiment, whereby **P5** was incubated at 65 °C in DMSO-d_6/D_2O (9 : 1) without irradiation, showed no degradation over at least 1 h (ESI, Fig. S72†), confirming that degradation of the PEtG backbone was initiated by UV-induced cleavage of the SIT end-group. Degradation of **P5** proceeded much more slowly than **P4a–b**, reaching a limiting degree of depolymerization of 50–60% after ~10 h. The slower rate and incomplete degradation of **P5** is consistent with putative hemiaminal formation, which is irreversible in the absence of a competing base such as morpholine (see ESI section S10.2† for auxiliary discussion). Nonetheless, degradation of **P5** demonstrates successful introduction of a cleavable *o*-nitrobenzyl cap *via* PSM and demonstrates that the SIT linker can undergo self-immolation without additional base, which has not previously been shown with this linker design.

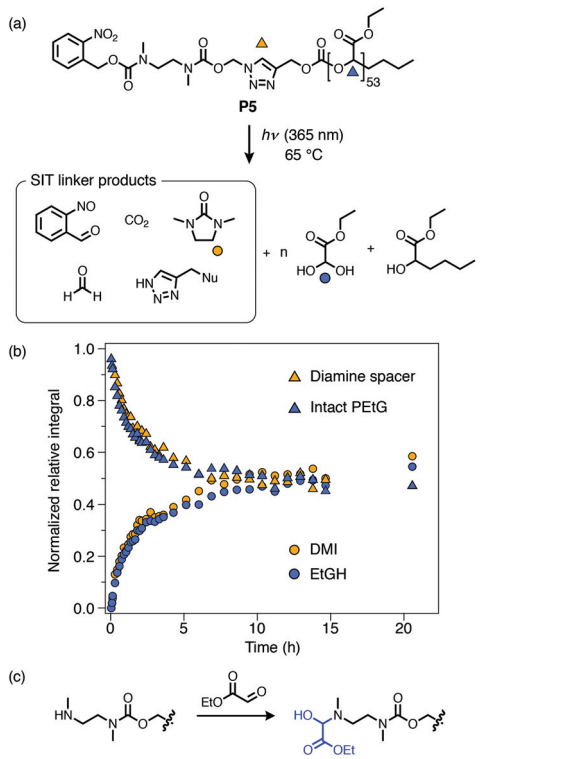

Scheme 8 Degradation analysis of *o*-nitrobenzyl capped **P5**. (a) Proposed degradation pathway. Markers denote the proton environments monitored in (b). 'Nu' denotes a generic nucleophilic residue, most likely –OH under these conditions. (b) Degradation kinetics profile following irradiation at 365 nm, measured by ^{1}H NMR analysis (~10 mmol in DMSO-d_6/D_2O 9 : 1, 65 °C) (full data shown in ESI, section S9.4†). (c) Proposed amine passivation mechanism, whereby liberated EtGH reacts with the deprotected cyclization spacer to form a hemiaminal when no other sacrificial nucleophiles are present (*e.g.*, morpholine, which was present for self-immolation experiments using **P4a–b**).

Conclusions

In conclusion, we have demonstrated a new method for the post-polymerization attachment of SIT end-groups to PEtG SIPs using the CuAAC reaction. Our approach involves the reaction of alkyne-terminated PEtGs with a dual-protected diamine precursor (**A**) carrying a cleavable carbamate 'trigger' group and an azidomethyl carbamate 'click' handle. Degradation profiles of the SIT-capped PEtGs and related small molecule model compounds were analyzed by *in situ* NMR spectroscopy experiments. Our results demonstrate that the ability of the SIT linker to undergo complete degradation depended strongly on the moiety connecting the SIT linker to the PEtG backbone. When this bridging group was an acetal, the SIT linker could not undergo 1,4-elimination, preventing depolymerization of the PEtG. However, when the bridging group was a carbonate, 1,4-elimination across the triazole ring proceeded rapidly, leading to successful degradation of the PEtG. Interestingly, unlike in previous work, kinetic profiles of the carbonate-bridged compounds showed that degradation of the SIT linker was not strongly influenced by substitution at the triazole Cα-position, as the diamine cyclization was the rate limiting step in the reaction sequence. We anticipate that, instead of tuning the end-cap cleavage rate using the triazole Cα-position, rate tuning can likely still be achieved by tuning the rate-limiting cyclization step through the incorporation of different cyclization spacers. Overall, the approach described herein can be used to introduce a variety of stimuli-responsive trigger groups to pre-synthesized SIPs *via* post-polymerization 'click' modification and may offer a new route for introducing self-immolative triazole junctions into polymer architectures.

Author contributions

PGM, XL, AH, OA, ALK, YCL, TNF and HZ performed synthesis, characterization, and data analysis. DAR performed self-immolation kinetics experiments. ERG and DAR designed and supervised the project. All authors assisted in preparation of the manuscript and ESI.

Conflicts of interest

There are no conflicts to declare.

Acknowledgements

The authors acknowledge financial support from the Australian Research Council (DE190100797), the Australian Academy of Science Regional Collaborations Programme, and the Natural Sciences and Engineering Research Council of Canada (Discovery Grant 2016-04636). The authors also acknowledge the facilities and the scientific and technical assistance of Sydney Analytical, a core research facility at the University of Sydney. We thank Dr Ian Luck (NMR) and Dr Nicholas Proschogo (MS) for technical assistance, and Dr Karen Hakobyan for maintenance of the analytical SEC systems.

Notes and references

1 R. E. Yardley, A. R. Kenaree and E. R. Gillies, *Macromolecules*, 2019, **52**, 6342–6360.
2 M. E. Roth, O. Green, S. Gnaim and D. Shabat, *Chem. Rev.*, 2015, **116**, 1309–1352.
3 G. I. Peterson, M. B. Larsen and A. J. Boydston, *Macromolecules*, 2012, **45**, 7317–7328.
4 S. Tang, L. Tang, X. Lu, H. Liu and J. S. Moore, *J. Am. Chem. Soc.*, 2018, **140**, 94–97.
5 Z. Deng, Y. Qian, Y. Yu, G. Liu, J. Hu, G. Zhang and S. Liu, *J. Am. Chem. Soc.*, 2016, **138**, 10452–10466.
6 J. Tan, Z. Deng, G. Liu, J. Hu and S. Liu, *Biomaterials*, 2018, **178**, 608–619.
7 X. Wang, C. Yao, G. Zhang and S. Liu, *Nat. Commun.*, 2020, **11**, 1524.
8 Y. Xiao, X. Tan, Z. Li and K. Zhang, *J. Mater. Chem. B*, 2020, **8**, 6697–6709.
9 M. T. Gambles, B. Fan, A. Borecki and E. R. Gillies, *ACS Omega*, 2018, **3**, 5002–5011.
10 M. Gisbert-Garzaran, D. Lozano, M. Vallet-Regi and M. Manzano, *RSC Adv.*, 2017, **7**, 132–136.
11 S. M. Heuchan, B. Fan, J. J. Kowalski, E. R. Gillies and H. A. L. Henry, *J. Agric. Food Chem.*, 2019, **67**, 12720–12729.
12 S. M. Heuchan, J. P. MacDonald, L. A. Bauman, B. Fan, H. A. L. Henry and E. R. Gillies, *ACS Omega*, 2018, **3**, 18603–18612.
13 M. S. Baker and S. T. Phillips, *Org. Biomol. Chem.*, 2012, **10**, 3595–3599.
14 S. Gnaim and D. Shabat, *Acc. Chem. Res.*, 2019, **52**, 2806–2817.
15 R. Weinstain, P. S. Baran and D. Shabat, *Bioconjugate Chem.*, 2009, **20**, 1783–1791.
16 K. Yeung, H. Kim, H. Mohapatra and S. T. Phillips, *J. Am. Chem. Soc.*, 2015, **137**, 5324–5327.
17 E. M. Lloyd, H. Lopez Hernandez, E. C. Feinberg, M. Yourdkhani, E. K. Zen, E. B. Mejia, N. R. Sottos, J. S. Moore and S. R. White, *Chem. Mater.*, 2018, **31**, 398–406.
18 M. S. Baker, H. Kim, M. G. Olah, G. G. Lewis and S. T. Phillips, *Green Chem.*, 2015, **17**, 4541–4545.
19 A. Sagi, R. Weinstain, N. Karton and D. Shabat, *J. Am. Chem. Soc.*, 2008, **130**, 5434–5435.
20 R. Erez and D. Shabat, *Org. Biomol. Chem.*, 2008, **6**, 2669–2672.
21 S. Gnaim and D. Shabat, *Acc. Chem. Res.*, 2014, **47**, 2970–2984.
22 M. G. Olah, J. S. Robbins, M. S. Baker and S. T. Phillips, *Macromolecules*, 2013, **46**, 5924–5928.
23 X.-W. Kan, L.-J. Zhang, Z.-Y. Li, F.-S. Du and Z.-C. Li, *Macromol. Rapid Commun.*, 2021, 2100169.
24 E. K. Y. Chen, R. A. McBride and E. R. Gillies, *Macromolecules*, 2012, **45**, 7364–7374.
25 K. Kumar and A. P. Goodwin, *ACS Macro Lett.*, 2015, **4**, 907–911.
26 J. M. Lobez and T. M. Swager, *Angew. Chem., Int. Ed.*, 2010, **49**, 95–98.
27 O. P. Lee, H. Lopez Hernandez and J. S. Moore, *ACS Macro Lett.*, 2015, **4**, 665–668.
28 B. Fan, J. F. Trant, A. D. Wong and E. R. Gillies, *J. Am. Chem. Soc.*, 2014, **136**, 10116–10123.
29 C. E. Diesendruck, G. I. Peterson, H. J. Kulik, J. A. Kaitz, B. D. Mar, P. A. May, S. R. White, T. J. Martínez, A. J. Boydston and J. S. Moore, *Nat. Chem.*, 2014, **6**, 623–628.
30 R. Weinstain, A. Sagi, N. Karton and D. Shabat, *Chem. – Eur. J.*, 2008, **14**, 6857–6861.
31 Y. Xiao, Y. Li, B. Zhang, H. Li, Z. Cheng, J. Shi, J. Xiong, Y. Bai and K. Zhang, *ACS Macro Lett.*, 2019, **8**, 399–402.
32 Y. Xiao, H. Li, B. Zhang, Z. Cheng, Y. Li, X. Tan and K. Zhang, *Macromolecules*, 2018, **51**, 2899–2905.
33 R. E. Yardley, A. Rabiee Kenaree, X. Liang and E. R. Gillies, *Macromolecules*, 2020, **53**, 8600–8609.
34 Q. E. A. Sirianni, A. Rabiee Kenaree and E. R. Gillies, *Macromolecules*, 2018, **52**, 262–270.
35 B. Fan and E. R. Gillies, *Mol. Pharm.*, 2017, **14**, 2548–2559.
36 G. Liu, X. Wang, J. Hu, G. Zhang and S. Liu, *J. Am. Chem. Soc.*, 2014, **136**, 7492–7497.
37 G. Liu, G. Zhang, J. Hu, X. Wang, M. Zhu and S. Liu, *J. Am. Chem. Soc.*, 2015, **137**, 11645–11655.
38 R. M. Arnold, N. E. Huddleston and J. Locklin, *J. Mater. Chem.*, 2012, **22**, 19357–19365.
39 K. A. Günay, P. Theato and H.-A. Klok, *J. Polym. Sci., Part A: Polym. Chem.*, 2013, **51**, 1–28.
40 Y. Zhong, B. J. Zeberl, X. Wang and J. Luo, *Acta Biomater.*, 2018, **73**, 21–37.
41 S. Tempelaar, L. Mespouille, O. Coulembier, P. Dubois and A. P. Dove, *Chem. Soc. Rev.*, 2013, **42**, 1312–1336.
42 D. A. Roberts, T. W. Schmidt, M. J. Crossley and S. Perrier, *Chem. – Eur. J.*, 2013, **19**, 12759–12770.
43 G. Gody, D. A. Roberts, T. Maschmeyer and S. Perrier, *J. Am. Chem. Soc.*, 2016, **138**, 4061–4068.

44 D. A. Roberts, B. S. Pilgrim, T. N. Dell and M. M. Stevens, *Chem. Sci.*, 2020, **11**, 3713–3718.
45 T. N. Forder, P. G. Maschmeyer, H. Zeng and D. A. Roberts, *Chem. – Asian J.*, 2021, **16**, 287–291.
46 A. Rabiee Kenaree and E. R. Gillies, *Macromolecules*, 2018, **51**, 5501–5510.
47 C. A. Blencowe, D. W. Thornthwaite, W. Hayes and A. T. Russell, *Org. Biomol. Chem.*, 2015, **13**, 8703–8707.
48 J. Gordon, *2-Methylbut-3-yn-2-ol in Encyclopedia of Reagents for Organic Synthesis*, 2001. DOI: 10.1002/047084289X.rm157.